Electronic Supplementary Material (ESI) for Lab on a Chip

Filtering Microfluidic Bubble Trains at a Symmetric Junction.

Electronic Supplementary Information

Pravien Parthiban

Department of Chemical and Biomolecular Engineering,

National University of Singapore, 4 Engineering Drive 4, E5-02-28, Singapore 117576

Saif A Khan*

Singapore-MIT Alliance, National University of Singapore,

4 Engineering Drive 3, E4-04-10, Singapore 117576 and

Department of Chemical and Biomolecular Engineering,

National University of Singapore, 4 Engineering Drive 4, E5-02-28, Singapore 117576

*chesakk@nus.edu.sg

I. MEASURING CHANNEL HEIGHT AND TESTING THE SYMMETRY OF THE LOOP

To measure the channel heights in both arms of the loop, a PDMS replica of the microfluidic loop was first molded. Slices of the channel were cut carefully, and a digital micrograph of the cross-section was obtained using a CCD camera (Basler pi640) mounted on a stereomicroscope (Leica MZ16). A total of 16 digital micrographs at different positions along the length of each arm of the loop were obtained. The height of the channel was subsequently measured manually from the micrographs using the *Measure Tool* in Adobe Photoshop. The average height in arm 1 was $123.2\mu m$ whilst that in arm 2 was $122.6\mu m$ (the standard deviations for the measured heights of both arms was less than $1\mu m$).

This difference in height results in only a 1% difference in the resistance between both arms of the loop.(The ratio of the resistances of the arms of the loop ${}^0R_2/{}^0R_1 = [h_1^3(1 - 0.63h_1/w)]/[h_2^3(1-0.63h_2/w)] = 1.01$, where ${}^0R_i$ is the resistance of arm i when it contains no droplets/bubbles [1]).This 1% difference in resistance is not significant as typical asymmetric loops/junctions used for filtering droplet trains requires at least a 10%-50% difference in the resistance [2].

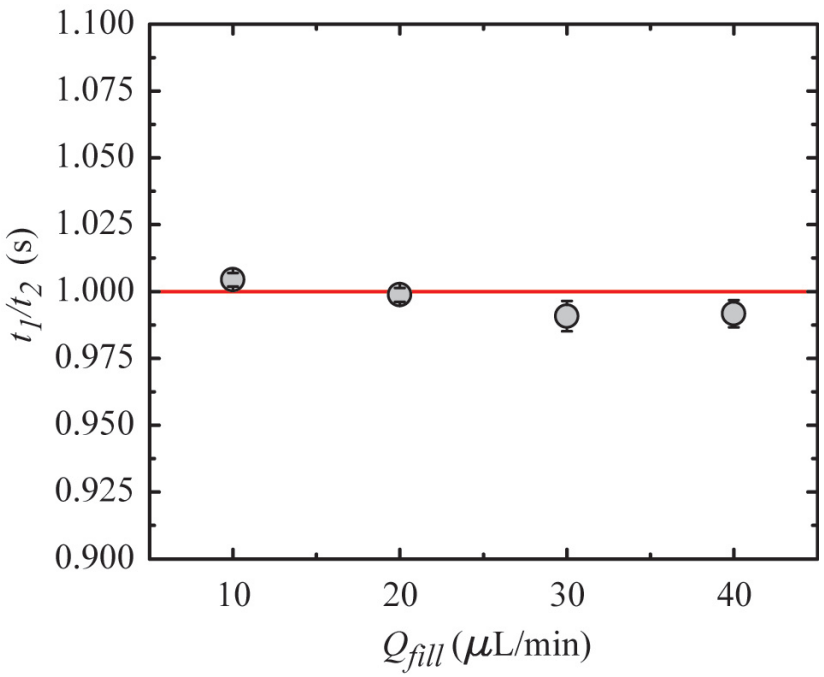

Fig S 1. Ratio of time required to fill arm 1 (t_1) to the time required to fill arm 2 (t_2) is nearly 1

We further test the symmetry of the loop by measuring the time taken to fill both arms of the loop with ethanol. We pump ethanol through the main liquid inlet (both the gas inlet and secondary liquid inlet are left unused) of an empty microfluidic device at a flow rate Q_{fill} using a syringe pump, and capture videos of gas-liquid interface propagating through both arms of the loop at 100 fps as it is filled with ethanol. The videos are subsequently analyzed to determine the time required to fill arm 1 (t_1) and arm 2 (t_2) of the loop. Q_{fill} was varied between $10 - 40\mu L$ and each measurement was repeated twice. The results plotted in Figure S1 show that time to fill both arms of the loop are nearly identical, with t_1/t_2 varying between $0.990 - 1.00$ suggesting that the difference in heights is not significant.

II. MEASURING NUMBER OF BUBBLES (n), BUBBLE LENGTH (l_B) BUBBLE VELOCITY (U) AND LIQUID SLUG LENGTH (l_S)

The details of the bubble train flow in both the single microchannel used to measure the pressure drop and the symmetric microfluidic loop were captured by a video camera (Basler pi640) mounted on a stereo microscope (Leica MZ16). The videos of the flow were exported as a sequence of grayscale images which were subsequently analyzed to determine l_B, l_S, and U using an in house MatLab program. The field of view captured in the single microchannel device included 6 lanes of the channel (Figure S2 a). In the symmetric loop, the field of view included both the inlet to the loop and the lane upstream of it (Figure S2 f). The grayscale images were first converted into binary images using inbuilt MatLab functions (Figure S2 b and g). The resulting binary images are stored as a 2 dimensional matrix composed of ones (White) and zeros (Black). These binary images were cropped to obtain the region of interest, i.e the lane at which measurements are to be made (Figure S2 c and h). The cropped binary images were further digitized by performing a column wise scan to determine the location of the top edge of all the bubbles present (Figure S2 d and i). For each column the row number at which the first white to black transition occurred was stored. (In columns where no white to black transition occurred, a value of zero was stored). The resultant digitized signal possessed all relevant information regarding the axial positions of the bubbles (signal value>0) and liquid slugs (signal value$=0$). The location of the back and front caps of the bubbles were determined by scanning the digitized signal for transitions from a zero to a non zero value and vice versa. The bubble and liquid slug

lengths were then directly measured (in pixel units) from the locations of the back and front caps of the bubbles (Figure S2 d and i). To measure the velocity of the bubble, the position of the front cap of a bubble from the left edge of the image, $x(t)$, was measured for every frame as the bubble traversed across the field of view (Figure S2 e and j). The velocity of the bubble was subsequently determined (in units of pixels/s) as the slope (m) of the line $x(t) = mt + c$. The pixel units were converted to length units by first measuring the channel width ($w = 300\mu m$) in pixel units (using Adobe Photoshop) and then using it as a conversion factor. The number of bubbles (n) present in a microchannel of length L was calculated as $n = L/(l_B + l_S)$

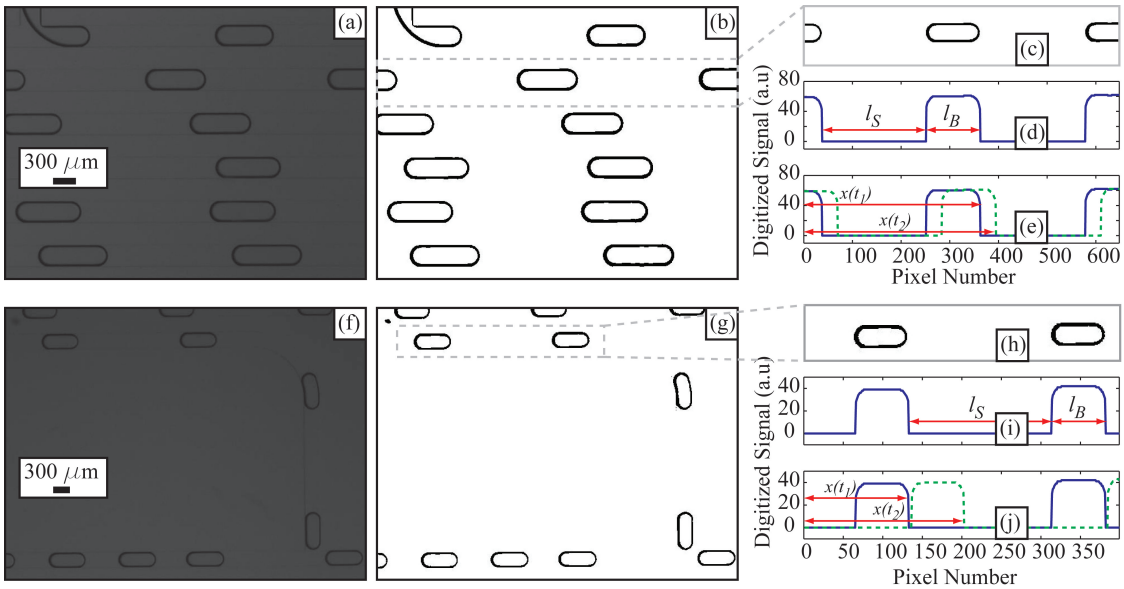

Fig S 2. Micrographs showing bubble train flow in the single channel device used for measuring pressure drop (a) and through the symmetric loop (f). (b,g) Binary images of the grayscale micrographs shown in *(a)* and *(f)* respectively. (c,h) Cropped binary images showing the region of interest. (d,i) Plot of the digitized signal obtained by column wise scanning of the cropped binary images to locate the top edges of the bubbles. The resultant digitized signal shows the axial location of the bubble (value> 0) and liquid slugs (value= 0) in the cropped images. The red lines indicate how l_B and l_S are measured (in pixel units) from the digitized signal. (e,j) Digitized signal from two micrographs captured at t_1 and t_2 are plotted, here $t1 - t2 = 0.025s$. $x(t)$ is the axial position (in pixel units) of the front cap of the bubble from the left edge of the image. The slope of line obtained by plotting $x(t)$ vs t gives the bubble velocity (in units of pixels/sec)

III. DETAILED DERIVATION OF THE EQUATION FOR HYDRODYNAMIC RESISTANCE OF A MICROCHANNEL CONTAINING BUBBLES

The hydrodynamic resistance of arm i containing n_i bubbles of length l_B is,

$$^{n_i}R_i = R_0[1-\phi] + n_i R_B \tag{1}$$

where R_0 is the hydrodynamic resistance of the arm completely filled with the continuous phase, ϕ is the fraction of the arm occupied by bubbles and R_B is the resistance to flow caused by a single bubble moving with a speed U_i.

$$\phi = \frac{n_i l_B}{L} \tag{2}$$

For channels of rectangular cross-section where $h < w$,

$$R_0 = \frac{12\mu L}{h^3 w(1-0.63h/w)} = \alpha L. \tag{3}$$

R_B in turn can be expressed as $R_B = \triangle P_B/(U_i wh)$, where $\triangle P_B$ is the pressure difference across the end caps of a confined bubble moving with a speed U_i through the microchannel. Therefore

$$R_B = 3.15\frac{2\sigma}{h}Ca_i^{2/3}\frac{1}{U_i wh} \tag{4}$$

substituting equations 2, 3 and 4 in equation 1 we have

$$^{n_i}R_i = \alpha L[1-\frac{n_i l_B}{L}] + n_i 3.15\frac{2\sigma}{h}Ca_i^{2/3}\frac{1}{U_i wh} \tag{5}$$

rearranging and simplifying we have

$$^{n_i}R_i = \alpha[L - n_i l_B] + n_i 3.15\frac{2\sigma}{h}Ca_i^{2/3}\frac{1}{U_i wh} \tag{6}$$

$$^{n_i}R_i = \alpha\left(L - n_i l_B + n_i 3.15\frac{2\sigma}{h}Ca_i^{2/3}\frac{1}{U_i wh}\frac{1}{\alpha}\right) \tag{7}$$

$$^{n_i}R_i = \alpha\left(L - n_i l_B + n_i 3.15\frac{2\sigma}{h}Ca_i^{2/3}\frac{1}{U_i wh}\frac{h^3 w(1-0.63h/w)}{12\mu}\right) \tag{8}$$

$$^{n_i}R_i = \alpha\left(L - n_i l_B + \frac{n_i \times 3.15 \times 2(1-0.63h/w)}{12}Ca_i^{2/3}\frac{\sigma}{\mu U_i}h\right) \tag{9}$$

$$^{n_i}R_i = \alpha \left(L - n_i l_B + n_i \times 0.389 \frac{Ca_i^{2/3}}{Ca_i} h \right) \tag{10}$$

thus the hydrodynamic resistance of arm i containing n_i bubbles of length l_B is,

$$^{n_i}R_i = \alpha \left[L - n_i l_B \left(1 - 0.389 \frac{h}{l_B Ca_i^{1/3}} \right) \right] \tag{11}$$

IV. EXPERIMENTAL MEASUREMENTS SHOWING THAT BUBBLES CAN LOWER THE HYDRODYNAMIC RESISTANCE TO FLOW IN MICROCHANNELS

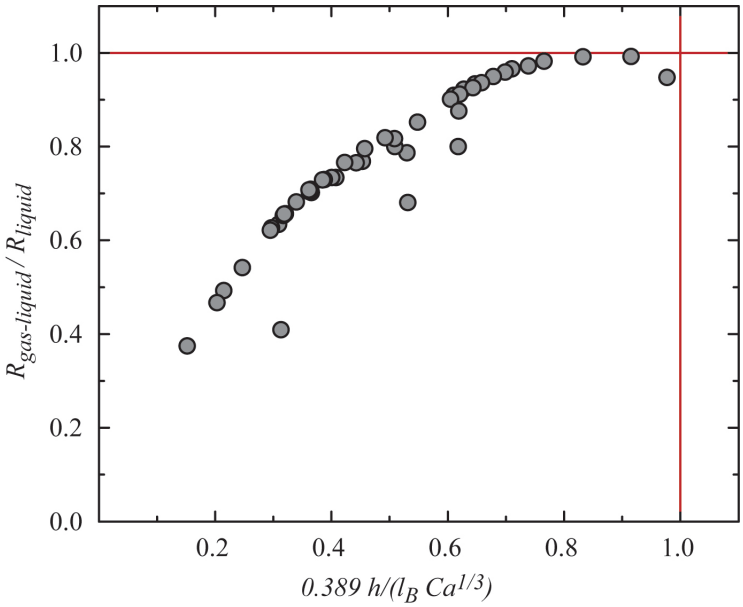

Fig S 3. The experimentally measured hydrodynamic resistance to flow in a microchannel containing bubbles $R_{gas-liquid}$ (measured from pressure drop experiments with the long microchannel) is less than the hydrodynamic resistance of the microchannel completely filled with liquid R_{liquid} when $0.389h/(l_B Ca^{1/3}) < 1$. This is exactly the same criteria for accessing the filter regime in experiments with the symmetric microfluidic loop. We plot here the ratio $R_{gas-liquid}/R_{liquid}$ against $0.389h/(l_B Ca^{1/3})$

The hydrodynamic resistance of a microchannel of length L containing n bubbles of length l_B is given by,

$$^{n}R = \alpha \left[L - n l_B \left(1 - 0.389 \frac{h}{l_B Ca^{1/3}} \right) \right] \tag{12}$$

Bubbles can lower the resistance to flow when $0.389h/(l_B Ca^{1/3}) < 1$. In this section we test this hypothesis experimentally. The hydrodynamic resistance to flow in a microchannel containing bubbles $R_{gas-liquid}$ can be calculated from the experimentally measured pressure drop (using the long microchannel) $\triangle P$, and bubble velocity U.

$$R_{gas-liquid} = \frac{\triangle P}{Q} = \frac{\triangle P}{U_i wh} \tag{13}$$

The hydrodynamic resistance of the microchannel completely filled with liquid is given by

$$R_{liquid} = \frac{12\mu L}{h^3 w(1 - 0.63h/w)} \tag{14}$$

We see that our experimentally measured $R_{gas-liquid}$ is indeed less than R_{liquid} when $0.389h/(l_B Ca^{1/3}) < 1$ (Figure S3). This is the same criteria for accessing the filter regime in experiments with the symmetric microfluidic loop.

---

[1] H. Bruus, *Theoretical Microfluidics* (Cambridge University Press, 1982) p. 51.

[2] D. A. Sessoms, M. Belloul, W. Engl, M. Roche, L. Courbin, and P. Panizza, Phys. Rev. E **80**, 016317 (2009).